ONE-NUCLEON $A \to A-1+N$ FRAGMENTATION OF NUCLEI WITH $A=7$

N.A. Burkova, K.A. Zhaksybekova, M.A. Zhusupov
Al-Farabi Kazakh National University,Tole be 96, Almaty, Kazakhstan, 050012

In recent review the most essential results of the potential cluster theory for two-body photodisintegration of light nuclei have been reported [1]. It was shown, that within the *binary* cluster presentation of $\alpha-$clusterized nuclei like $^6Li\{\alpha d\}$, $^7Li\{\alpha t\}$, $^7Be\{\alpha\tau\}$ and etc. practically all available experimental data with nonpolarized and linearly polarized photons were reproduced, as well as the qualitative interpretation of the corresponding observables was implemented on the microscopic level.

New development of this theory deals with a treatment of ^9Be fragmentation in two-cluster strongly binding channels, i.e. $^{6,7,8}Li+"c"$ [2]. The special feature concerns the construction of final channel cluster configurations which *do not coincide* with the initial $2\alpha n-$presentation of ^9Be according the multicluster dynamic model with Pauli projection (MDMP), *Kukulin et al* [3]. The results turned to be really successful, as all experimental data on the photodisintegration processes $^9Be(\gamma,p_{0+1})^8Li$, $^9Be(\gamma,d_{0+1})^7Li$, $^9Be(\gamma,t)^6Li$, $^9Be(\gamma,\tau)^6He$ and $^7Li(d,\gamma)^9Be$ have been reproduced [4]. Actually, it is interesting to apply this method to one-nucleon $A \to A-1+N$ fragmentation of nuclei with $A=7$.

1. Within a cluster model approach the following one-nucleon fragmentation channels $^7Li\{\alpha t\} \to {}^6Li\{\alpha np\}+n$, $^7Li\{\alpha t\} \to {}^6He\{\alpha nn\}+p$, $^7Be\{\alpha\tau\} \to {}^6Li\{\alpha np\}+p$ and $^7Be\{\alpha\tau\} \to {}^6Be\{\alpha pp\}+n$ have been treated. The cluster configuration of the corresponding nucleus is pointed in braces. Residual nuclei $A=6$ have been treated both in ground and excited states.

For isobaric triplet $^6He-{}^6Li-{}^6Be$ MDMP functions have been used [5]. Isobaric doublet $^7Li-{}^7Be$ is described in a framework of $\alpha t-$ and $\alpha\tau-$cluster models based on the deep attractive potentials with excluded Pauli forbidden states [6]. It should be note, that in many particle shell model (MPSM) ^7Li and ^7Be nucleus are *indistinguishable*, but in cluster model they are *not identical*. Thus, it is not obvious, that ^7Li and ^7Be have one and the same spectroscopic characteristics as it follows from MPSM. This is a question for the following discussion.

It should be point, that in case of light nuclei *resultant isobars* $(Z-1,N+1)$ and $(Z+1,N-1)$ are unstable, but resemble the structure of a *parent* nucleus (Z,N). For example, ^6He is unstable long-live nucleus, $\tau_{1/2}=0{,}802$ s, ^6Be – unstable short-live nucleus, with life-time $\sim 10^{-21}$ s. *Hence, it is a challenge to find a way for getting information on short-living isobar using the data on the stable parent nucleus or on the more stable isobaric partner.*

Here the virtual decays $^7Li \to {}^6Li+n$, $^7Li \to {}^6He+p$, $^7Be \to {}^6Li+p$ and $^7Be \to {}^6Be+n$ of isobar analogous channels are treated in details. Corresponding excitation levels E_x of $^6He-{}^6Li-{}^6Be$ triplet are pointed in Table 1. The relative motion wave functions (WF) in final channels have been obtained analytically as a result of overlapping integration and were used for the calculation of neutron S_n- and proton S_p-spectroscopic factors [7,8]. Residual nuclei $A=6$ have been treated both in ground and excited states. Projecting procedure of $\alpha t-$ and $\alpha\tau-$cluster functions assumes the using of structural WF of t and τ nucleus. It is possible to use the parametrization corresponding to free nuclei. In our case we are doing with translational invariant shell model (TISM) for t and τ, what allows to vary the oscillator parameter r_0 and, thus to simulate the deformation of three-body cluster.

Table 1

$^{7}Li \to ^{6}Li + n$, $^{7}Li \to ^{6}He + p$				
j^{π},T	$0^{+},1$		$2^{+},1$	
A=6	^{6}Li	^{6}He	^{6}Li	^{6}He
E_x, MeV	3,56	$g.s.$	5,37	1,797
$S^{theor.}$ [9]	0,285	0,571	0,208	0,416
S^{theor} [10]		0,56		0,34
S^{exp} [11]	0,24	0,48 *	0,14	0,28 *
$S^{exp.}$ [12]	0,31 *	0,62	0,165(0,16) *	0,37 (0,32)
$S^{exp.}$ [13]	0,21 *	0,42(4)	0,08 *	0,16(2)
$S^{exp.}$ [14]	0,3*	0,6	0,2*	0,4
S^{theor}_{VMC} [13]		0,41		0,19
S^{theor}, r_0=1,3	0,2244	0,4611	0,1456	0,2913
S^{theor}, r_0=1,67	0,2855	0,5805	0,1688	0,3344
S^{theor}, r_0=2,36	0,2281	0,4563	0,1106	0,2189
$^{7}Be \to ^{6}Li + p$, $^{7}Be \to ^{6}Be + n$				
j^{π},T	$0^{+},1$		$2^{+},1$	
A=6	^{6}Li	^{6}Be	^{6}Li	^{6}Be
E_x, MeV	3,56	$g.s.$	5,37	1,67
S^{theor}, r_0=1,6	0,2865	0,5333	0,1748	0,3320
S^{theor}, r_0=1,8	0,2963	0,5588	0,1725	0,3317

* – *experimental data recalculated according model-independent ratio* S_p / S_n *=2*

The method of getting out the spectroscopic information on $^{7}Be \to ^{6}Be + n$ virtual decay cluster channel was suggested basing on comparative analyses with $^{7}Li \to ^{6}Li + n$ and $^{7}Li \to ^{6}He + p$ channels [7], as well as with $^{7}Li \to ^{6}Li + n$ and $^{7}Be \to ^{6}Li + p$ ones [8].

It was shown in [7,8] that S-factors in $^{7}Li \to ^{6}Li + n$ and $^{7}Li \to ^{6}He + p$ channels are correlated by model independent ratio (MIR) $R = S_p / S_n$. In MPSM $R = 2$ exactly. In cluster models *R* is varying within 3-4% range. So, data on proton S_p-factors may be recalculated into data on neutron S_n-factors and vice versa (Table 1). In case of $^{7}Li \to ^{6}Li + n$ and $^{7}Be \to ^{6}Li + p$ channels MIR was also found and it equals $R = S_p / S_n \sim 1$ [8]. As it is seen from Table 1, a comparison of the calculated $S-$ factors with available experimental data as well as with theoretical calculations done within a traditional many-particle shell model shows no radical discrepancies, and, even more, are in good agreement.

2. The developed approach was applied to treating of $^{7}Li+\gamma \rightleftarrows {}^{6}He+p$ processes. For direct photodisintegration reaction $^{7}Li(\gamma,p_{0+1})^{6}He$ two groups of experimental data on integral [15] and differential [16] cross sections measured from threshold up to E_{γ}~30 MeV more than 30 years ago are known. The problem is that these data are not in concordance. Exclusive data on $^{7}Li(\gamma,p_{0})^{6}He$ in energy interval $E_{\gamma}\sim 50-140$ MeV are also available [17], but they are out of the frame of potential approach.

So, in present calculations we orient on radiative proton capture $^{6}He(p,\gamma_{0+1})^{7}Li$ data measured recently in inverse kinematics [18]. As in experiment transitions into g.s. of $^{7}Li(3/2^{-})$ and 1-st exc. state $1/2^{-}$ (0,48 MeV) are indistinguishable, the following amplitudes have been taken into account in present calculations:

$$s(1/2^{+})+d(3/2^{+},5/2^{+})\xrightarrow{E1}P_{g.s.,3/2} \quad (1) \qquad s(1/2^{+})+d(3/2^{+})\xrightarrow{E1}P_{exc,1/2} \quad (3)$$
$$p(1/2^{-},3/2^{-})+f(5/2^{-},7/2^{-})\xrightarrow{E2}P_{g.s.,3/2}; \quad (2) \qquad p(3/2^{-})+f(5/2^{-})\xrightarrow{E2}P_{exc,1/2}. \quad (4)$$

Fig. 1*a* shows a comparison of our calculations and those done [18] within the resonating group method (RGM). RGM calculations are normalized to the data and accounted only E1-multipole. One may recognize that our results reproduce the experiment better comparing RGM.

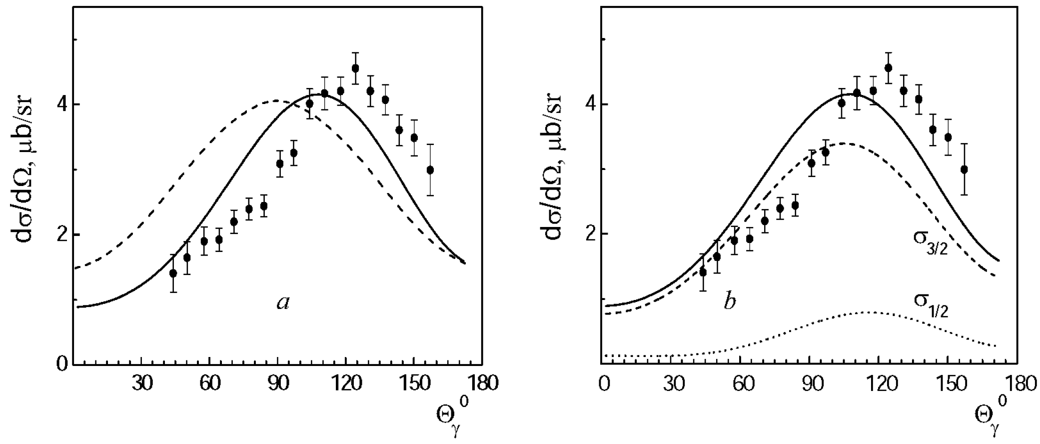

Fig. 1. Angular distributions in the process $^{6}He(p,\gamma_{0+1})^{7}Li$. Exp. – [18]. *a* – comparison of present (solid) and RGM [18,19] (dash) calculations; *b* – partial $\sigma_{3/2}$ and $\sigma_{1/2}$ cross sections, present work

One more essential difference of present work and RGM concerns estimations of relative input of partial cross sections $\sigma_{3/2}$ and $\sigma_{1/2}$ into angular distributions at $E_{\gamma}=40$ MeV (Fig.1). According Table 2 from RGM calculations the ratio $\sigma_{1/2}/\sigma_{3/2}=2,9$ follows. Authors [18] used this value for estimation of absolute value of experimental integral cross section $\sigma_{\exp}=35\pm 2$ μb. Using data on photodisintegration $^{7}Li(\gamma,p_{0})^{6}He$ [17] via detailed balance consideration a value $\sigma_{3/2}=9,6\pm 0,4\,\mu b$ was obtained for transitions to $^{7}Li_{g.s.}$. Then, using factor 2,9 cross section $\sigma_{1/2}$ was calculated and final value $\sigma\sim 38$ μb was obtained. But, it should be noted that experimental data on $^{7}Li(\gamma,p_{0})^{6}He$ correspond to the photon energies $E_{\gamma}\geq 50$ MeV [17], thus it is not correct to use them in such a context.

Table 2

cross sections	$\sigma_{3/2}$, μb	$\sigma_{1/2}$, μb	σ, μb
theory [18]	15	44	59
present theory	31,08	6,0	37,08
exp. [17]	$9{,}6 \pm 0{,}4$	-	~38
exp. [18]	-	-	35 ± 2

Our estimations give $\sigma_{1/2} / \sigma_{3/2} = 0{,}19$ or inverse ratio $\sigma_{3/2} / \sigma_{1/2} = 5{,}2$, what differs from RGM. From Table 2 also well seen that our calculations reproduce the absolute value of the observed cross section very good. While $\sigma_{3/2}$ dominates, experimental data may be reproduced only if ~16% input of $\sigma_{1/2}$ cross section. That is why multipole analysis of both partial cross sections presented on Fig. 2 has a sense.

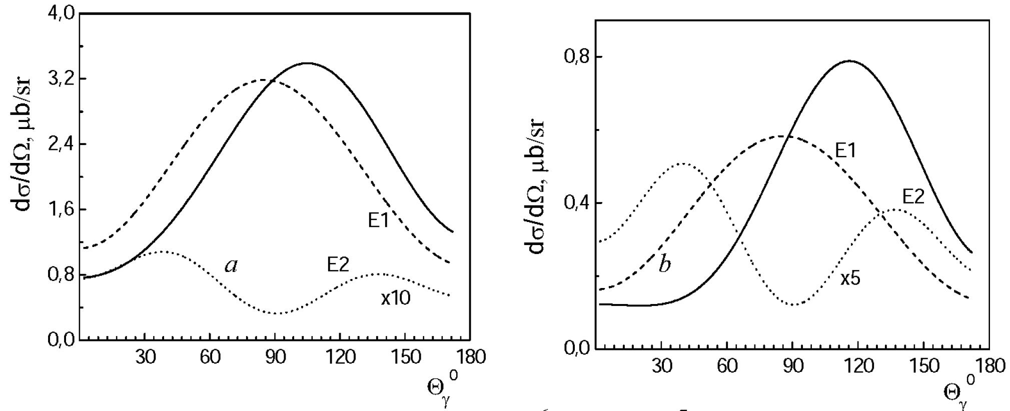

Fig. 2. Multipole cross sections of radiative capture $^6He(p,\gamma_{0+1})^7Li$: a – transitions to g.s., $\sigma_{3/2}$; b – transitions to 0,48 state, $\sigma_{1/2}$

Fig. 2 shows "forward-backward" asymmetry of both cross sections, but in case of $\sigma_{1/2}$ it is more pronounced. The reason of such a behavior is due to E1-E2 interference. So, more accurate specifying of V_{p^6He} interaction potential for *even* scattering waves may improve the description of experiment.

Basing on the same model, the calculation of integral cross section for the photodisintegration process $^7Li(\gamma,p_0)^6He$ was carried out, Fig. 3. Data sets (I and II refer to measurements with real photons corresponding to $E_{\gamma\max} = 28$ and 50 MeV, i. e. set II may include besides channel $^7Li(\gamma,p)$, Q=9,98 MeV, also channels $^7Li(\gamma,p2n)$, Q=10,95 MeV and $^7Li(\gamma,pn)$, Q=11,84 MeV [16].

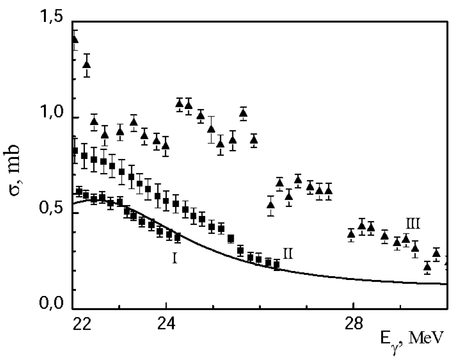

Fig. 3

The upper experimental points on Fig. 3 (III) were measured with real photons also and related to the process $^7Li(\gamma,p_{0+1})^6He$ [15]. Well seen that set (III) reveals the resonance energy dependence contrary to sets (I) and (II). Our calculations are done for the $^7Li(\gamma,p_0)^6He$ reaction and may be compared with set (I) only – a coincidence of theory and experiment is quite well.

As both experimental (set I) and calculated cross sections of photoreaction $^7Li(\gamma,p_0)^6He$ show monotonous energy dependence, one may explain the resonance structure of data set (III) by additional contribution of (γ,p_1)-channel corresponding to formation of ^{6}He nucleus in 1-st excited state $2^{+},1$. According our estimations in fragmentation channel $^{7}Li_{gs} \to ^{6}He(2^{+},1)+p$ states with channel spin $s_c = 5/2$ dominate absolutely comparing those with $s_c = 3/2$ [7,8]. This may lead to complicated final interactions $^{6}He(2^{+},1)+p$ what very likely was observed by *Denisov* [15]. Today there are no data on the high-spin states on proton fragmentation of ^{7}Li nucleus. Thus, new theoretic and experimental investigations of this problem are of great importance.

3. The developed approach for construction of $^{6}Li+n$-channel by means of projecting procedure $\left\langle ^{6}Li\{\alpha np\},n \middle| ^{7}Li\{\alpha t\}\right\rangle$, but the ***modified version***, was used for the calculation of $^{7}Li(\gamma,n)^{6}Li$ photodisintegration process at the energies E_γ~8-9 MeV. This energy range corresponds to (γ,n_0)-channel, i.e. experimental data might be recognized the exclusive ones [20,21]. Besides, there is an evidence of low-energy magnetic M1-resonace corresponding the $J_i^{\pi},T_i = 5/2^{-},1/2$ (7,456 MeV) level in ^{7}Li nucleus, which reveals also in continuous scattering $^{6}Li+n$-channel as a resonant behavior of p – phase shift.

Let us comment the modifications appeared in our model. In case of *direct* projecting we obtained the radial relative motion $^{6}Li_{g.s.}n$ bound state WF in a form

$$R^{(\kappa)}_{1^{+},s_c}(R_{6n}) = \alpha_{[000,1]}P^{2}_{[000,1]} + \alpha_{[022,1]}P^{4}_{[022,1]} + \beta_{[022,1]}F^{4}_{[022,1]} \tag{5}$$

Weight of each component equals the square root from the corresponding spectroscopic $S_{\kappa s_c}$ – factor: $\alpha_{[000,1]} = 0,97$, $\alpha_{[022,1]} = 0,74\cdot10^{-2}$, $\beta_{[022,1]} = 0,26\cdot10^{-2}$. In (5): κ–relative angular momentum; $[\lambda lL,S]$– partial components of ^{6}Li MDMP function [5]; s_C–channel spin. It is clear, that direct transitions $P^{2}_{[000,1]} \xrightarrow{M1} p_{s_s=3/2}(1/2^{-},3/2^{-},5/2^{-})$ to continuum with channel spin $s_s = 3/2$ are forbidden. Same problem met *Barker* [22], while performing the similar calculations basing on the ^{6}Lin-cluster model. But in our case it is possible to realize the modified scheme avoiding ***preliminary*** projection, but calculating the $\hat{\sigma}$-type matrix element $\left\langle ^{6}Li\{\alpha np\},n \middle| \hat{\sigma} \middle| ^{7}Li\{\alpha t\}\right\rangle$ directly. As a result, in case of M1-multipole transitions into $[\lambda lL,S] = [000,\ 1]$ state of ^{6}Li occurs and both spin channels s_C=1/2 and s_C=3/2 are allowed. Such a scheme gives rise for treating of ***magnetic*** disintegration $^{7}Li(\gamma,n)^{6}Li$ within the *direct mechanism* contrary to *Barker* approach, when Breit-Wigner formula for $\sigma_{res}(\gamma,n_0)$ cross section was used. Besides M1-multipole convective electric E1- and E2-multipoles (channel spin is conserved $s_s = s_c$) are accounted. So, the corresponding amplitudes are

$$P^{2}_{[000,1]} \xrightarrow{E1} s(1/2^{+}) + d(3/2^{+},5/2^{+}) \tag{6}$$

$$P^{2}_{[000,1]} \xrightarrow{E2} p(1/2^{-},3/2^{-}) + f(5/2^{-},7/2^{-}) \tag{7}$$

The results of present calculations and their comparison with available experimental data are presented on Fig. 4.

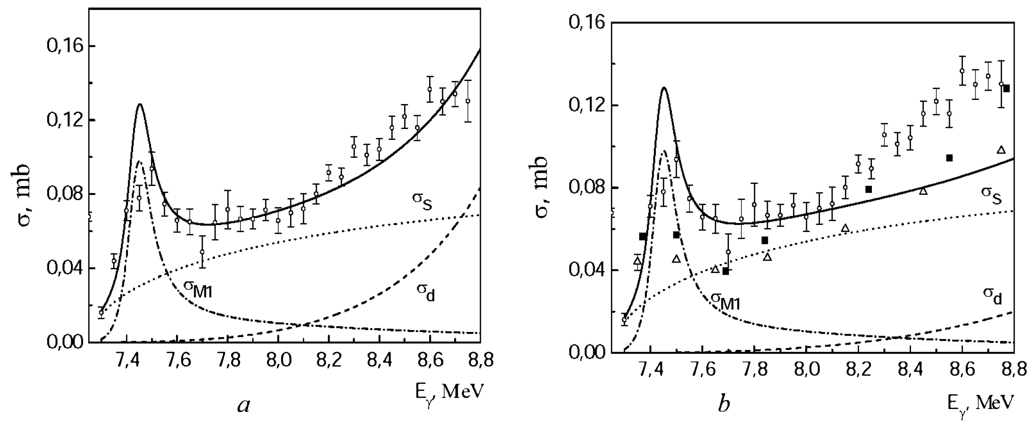

Fig. 4. Cross sections of the $^7Li(\gamma,n_0)^6Li$. Experiment: ○ – [21], – [23], △ - [24]. Theory: *a* – fit of data from [21], *b* – *realistic* calculations

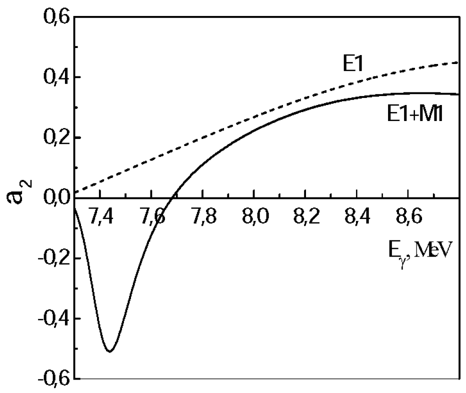

Fig. 5.

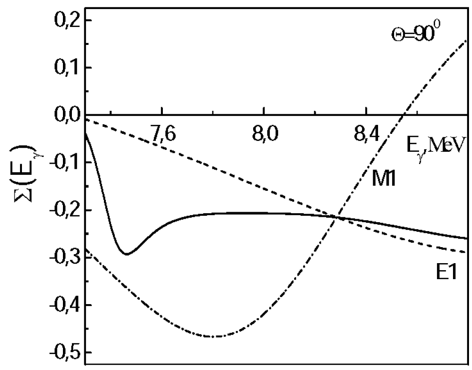

Fig. 6.

As it is seen from Fig. 4a we may fit the experimental data very accurately, but according our analysis more realistic calculations are presented at Fig. 4b, as preliminary treating of the higher E_γ-energies spectrum may be reproduced well with the parameters set for $V_{6_{Lin}}$ interaction potential corresponding Fig. 4b.

So, both *Barker*' and present report demonstrated that it is possible to *fit* the low-energy cross sections precisely, but the problem is that all experimental data being in qualitative coincidence differ quantitatively, and there is no independent criterion to make a reliable choice among them. *Thus, we suggest some additional characteristics for the possible new experimental investigations of the* $^7Li(\gamma,n)^6Li$ *process.*

As E2-multipole plays minor role within the treating energy interval, the angular distributions of the photoneutrons are determined by A_0 and a_2 coefficients in Legendre polynomial expansion. The corresponding energy dependence of a_2-coefficient presented on Fig. 5 shows specific illumination of M1-multipole on the background of E1-transition.

For comparison Fig. 6 illustrated the energy dependence of photoneutrons asymmetry $\Sigma(E_\gamma,\theta)$ in disintegration of ^7Li by linearly polarized photons $\vec{\gamma}$. It should be note that E1- and M1-amplitudes do not interfere.

In conclusion, we want remark, that simple binary αt – model may be successfully applied for the description of the one-nucleon spectroscopy as well as some aspects of (γ, N) photonuclear reactions.

REFERENCES

1. Burkova N. A., Zhaksybekova K.A., Zhusupov M. A. // Physics of Particles and Nuclei. 2005. V. 36. № 4. P. 427.
2. Burkova N. A., Zhaksybekova K.A., Zhusupov M. A. // Izv. RAN. Ser. Fiz. 2004. V. 68, № 8. P. 1203.
3. Kukulin V. I., Vorontchev V. T., Pomerantcev V.N. // Few-Body Syst. 1995. V. 18. P. 191.
4. Burkova N. A., Zhaksybekova K.A., Zhusupov M. A. // Izv. RAN. Ser. Fiz. 2005. V. 69, № 11. P. 1676; Izv. RAN. Ser. Fiz. 2006. V. 70, № 2. P. 280; ibid P. 314.
5. Kukulin V. I. et al. // Nucl. Phys. A. 1995. V.586. P. 151.
6. Dubovichenko S.B. Properties of light atomic nuclei in potential cluster model. Almaty, 2004. 247 p.
7. Burkova N.A., Zhaksybekova K.A. // Izv. NAN RK. Ser. Fiz.-mat. 2005. № 2(240). P.61; Vest. KazNU. Ser. fiz. 2005. № 1(19). P. 11, ibid C.16; Izv. RAN. Ser. Fiz. 2006. № 2. P. 309; Vest. KazNU. Ser. fiz. 2006. № 2(22). P. 14.
8. Zhaksybekova K.A. // Izv. NAN RK. Ser. Fiz.-mat. 2005. № 3(241). P.59; Vest. KazNU. Ser. fiz. 2005. № 1(19).P.156.
9. Boyarkina A.N. Structure of 1p-shell nuclei. Moscow: MSU, 1973. 62 p.
10. Barker F.C. // Nucl. Phys.1966. V. 83. P. 418.
11. Ajzenberg-Selove F. // Nucl. Phys. A. 1988. V. 490. P. 1.
12. Brady F.P., King N.S.P., Bonner B.E. et al. // Phys. Rev. C. 1977. V. 16, №1. P. 31.
13. Lapikas L., Wesseling J., and Wiringa R.B. // Phys. Rev. Lett. 1999. V. 82, №22. P. 4404; Nucl. Phys. A. 2000. V. 663 & 664. P. 377c.
14. Sakuta S.B. et al. // Yad. Fiz. 2002. V. 65, №10. P. 1819.
15. 15.Denisov V.P.,Kul'chitski L.A. // Yad. Fiz. 1966. V.3. P.192.
16. Junghans G., Bangert K. et al. // Z. Physik A. 1979. V. 291. P 353.
17. Sene M.R. et al. // Nucl. Phys. A. 1985. V. 442. P. 215.
18. Sauvan E. et al. // Phys. Rev. Lett. 2001. V. 87, N 4. P. 042501.
19. Arai K., Descouvemont P., Baye D. // Phys. Rev. C. 2001. V. 63. P. 044611.
20. Siddiqui S.A., Dytlewski N., Thies H.H. // Nucl. Phys. A. 1986. V. 458. P. 387.
21. Karataglidis S. et al. // Nucl. Phys. A. 1989. V.501. P. 108.
22. Barker F.C. // Aust. J. Phys. 1980. V. 33. P. 159.
23. Bramblett R.L. et al. // Proc. Int. Conf. Photonucl. React. Appl. California. 1973.V. 1. P. 175.
24. Ferdinande H., Sherman N.K., Lokan K.H., Ross. C.K. // Can. J. Phys. 1977. V. 55. P. 428.